ChemComm

COMMUNICATION

View Article Online
View Journal | View Issue

Cite this: *Chem. Commun.*, 2022, **58**, 13270

Received 11th October 2022,
Accepted 5th November 2022

DOI: 10.1039/d2cc05547c

rsc.li/chemcomm

Electronic, steric and catalytic properties of N-heterocyclic carbene rhodium(I) complexes linked to (metallo)porphyrins†

Ludivine Poyac,[a] Stefano Scoditti,[b] Xavier Dumail,[a] Michel Granier,[a] Sébastien Clément,[a] Rafael Gramage-Doria,[c] Charles H. Devillers[d] and Sébastien Richeter*[a]

Electronic and steric properties of NHC ligands functionalized with porphyrins were investigated. When porphyrins are used as NHC-wingtips, nickel(II) in the macrocyle significantly improves the catalytic activity of the neighbouring NHC-Rh(I) complex in the conjugate addition of phenylboronic acid to cyclohexen-2-one.

N-Heterocyclic carbenes (NHCs) are ubiquitous ligands in homogenous transition metal catalysis.[1] Rationalizing catalytic properties of NHC-metal complexes mainly consists in investigating electronic and steric properties of NHCs. Imidazol-2-ylidenes are among the most commonly used NHCs in catalysis. Their electronic properties are affected by the substituents on C4 and C5 atoms and by the wingtip groups on N1 and N3 atoms, while their steric properties are mainly affected by the size and the rigidity of the wingtip groups oriented toward the metal centre (Fig. 1).[2] Descriptors like Tolman electronic parameter (TEP) and percent of buried volumes (%V_{bur}) are routinely used to quantify electronic and steric properties of NHCs, respectively.[2,3]

Several NHCs linked to porphyrins were reported[4] and used in organocatalysis[5] and transition metal catalysis.[6] Here, we propose to investigate electronic, steric and catalytic properties of three types of NHC-Rh(I) complexes linked to porphyrins, namely **M^1-A-M^2**, **M^1-B-M^2** and **M^1-C-M^2**, where M^1 is the metal in the porphyrin core (2H, Zn or Ni) and M^2 is the outer Rh(cod)Cl (cod = 1,5-cyclooctadiene) or Rh(CO)$_2$Cl complex (Fig. 1). In complexes **M^1-A-M^2**, porphyrins and NHCs are separated by benzyl groups. In complexes **M^1-B-M^2**, porphyrins and NHCs are fused together and the C4 and C5 atoms of NHCs correspond to two neighbouring β-pyrrolic carbon atoms. This rigid structure ensures that the inner metal M^1 is remote from the outer metal M^2. In complexes **M^1-C-M^2**, porphyrins are wingtips of NHCs and both are linked together through the formation of C_{meso}–N_{NHC} bonds. In this case, inner metal M^1 and outer metal M^2 are in close proximity (~5–6 Å) and cooperativity between them may be observed. For example, the inner metal M^1 can be used as binding site to fix substrates near the peripheral catalytic site in order to increase catalyst activity and/or selectivity.[7] Finally, 1,3-dimethylimidazol-2-ylidene ligand **IMe** is used as reference NHC. (NHC)Rh(cod)Cl and (NHC)Rh(CO)$_2$Cl complexes were used to assess steric and electronic properties, respectively. Then, catalytic properties of (NHC)Rh(cod)Cl complexes were investigated for the conjugate addition of phenylboronic acid to cyclohexen-2-one.

Imidazolium salts used as NHC precursors were obtained following synthetic strategies depicted in Scheme 1. Imidazolium salts **M^1-A-Cl** were obtained by first synthesizing the free-base *meso* 5-(4'-chloromethylphenyl)-10,15,20-tris(mesityl)porphyrin **2H-1**.[8] SN reaction with *N*-methylimidazole afforded imidazolium salt **2H-A-Cl**. Then, metalation reactions afforded the corresponding Ni(II) and Zn(II) porphyrins (**Ni-A-Cl** and **Zn-A-Cl**). Imidazolium salts **M^1-B-BF$_4$**

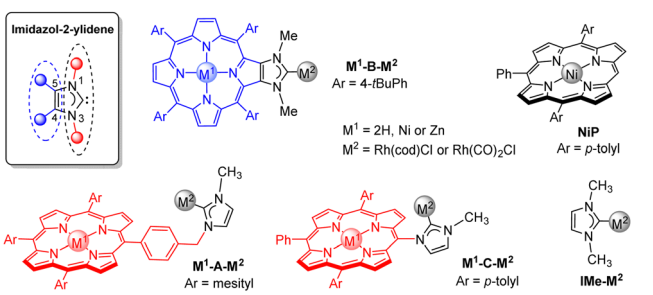

Fig. 1 Structures of complexes **M^1-B-M^2**, **M^1-B-M^2**, **M^1-C-M^2**, IMe-M^2 and NiP.

[a] *ICGM, Univ Montpellier, CNRS, ENSCM, Montpellier 34293, France. E-mail: sebastien.richeter@umontpellier.fr*
[b] *Department of Chemistry and Chemical Technologies, Univ of Calabria, Via P. Bucci, Rende 87036, Italy*
[c] *Univ Rennes, CNRS, ISCR-UMR 6226, Rennes, F-35000, France*
[d] *ICMUB UMR 6302, CNRS, Univ Bourgogne Franche-Comté, 9 avenue Alain Savary, Dijon 21078, France*

† Electronic supplementary information (ESI) available: Experimental details, synthetic procedures, NMR spectra, mass spectra, computational details and catalytic studies. See DOI: https://doi.org/10.1039/d2cc05547c

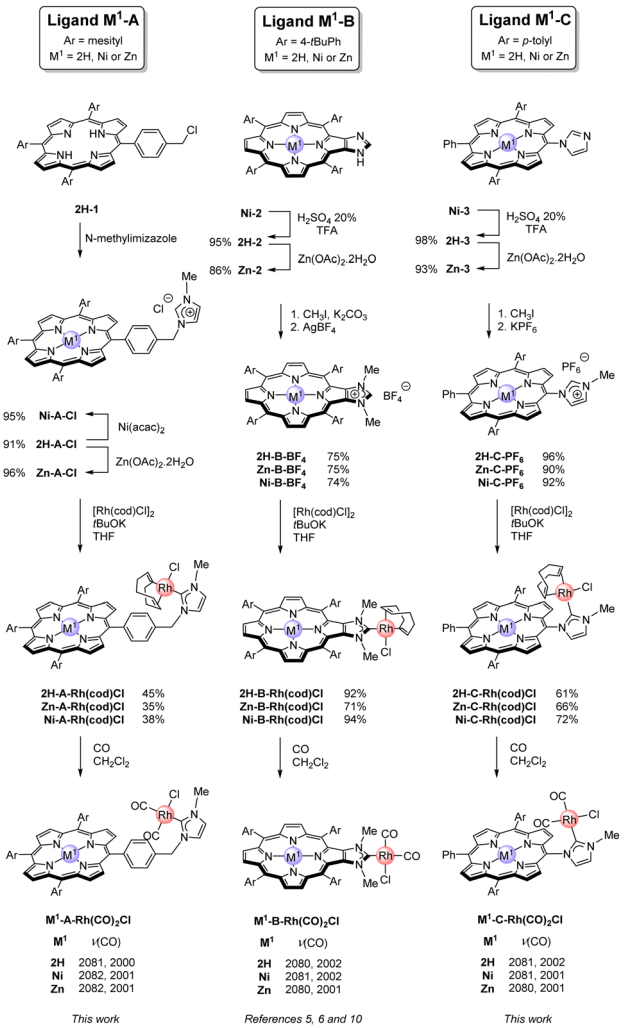

Scheme 1 Synthesis of Rh(I) complexes.

and **M^1-C-PF$_6$** were obtained by first synthesizing the corresponding Ni(II) porphyrins bearing an imidazole ring fused to a pyrrole (**Ni-2**) or on a *meso* position (**Ni-3**) following our reported procedures.[9] Then, demetalation (TFA/H_2SO_4 20%) and remetalation with Zn(II) afforded the corresponding free-base porphyrins (**2H-2** and **2H-3**) and Zn(II) porphyrins (**Zn-2** and **Zn-3**), respectively. SN reactions of these porphyrins with CH_3I and anion metathesis reactions afforded imidazolium salts **M^1-B-BF$_4$** and **M^1-C-PF$_6$** (M^1 = 2H, Ni or Zn). Complexes **M^1-A-Rh(cod)Cl**, **M^1-B-Rh(cod)Cl** and **M^1-C-Rh(cod)Cl** (M^1 = 2H, Ni or Zn) were obtained by reacting imidazolium salts with *t*BuOK and $[Rh(cod)Cl]_2$ (Scheme 1).[5,6,10] Formation of the C_{NHC}–Rh bonds was confirmed by the absence of the signals of the imidazolium protons in their ^{1}H NMR spectra and by the characteristic doublets observed at $\delta \sim 180$–190 ppm in their $^{13}C\{^1H\}$ NMR spectra. Characteristic signals due to coordinated cod ligands were also observed by ^{1}H NMR spectroscopy.

Measuring CO stretching wavenumbers of $(NHC)Rh(CO)_2Cl$ complexes by FTIR spectroscopy allowed to assess the electronic properties of NHCs and determine their TEP values.[11] Complexes **M^1-A-Rh(CO)$_2$Cl**, **M^1-B-Rh(CO)$_2$Cl** and **M^1-C-Rh(CO)$_2$Cl** were obtained by bubbling CO in solutions of the corresponding (NHC)Rh(cod)Cl complexes in CH_2Cl_2 (Scheme 1, these complexes were generated *in situ* and not isolated). Two CO stretching wavenumbers were observed in the FTIR spectra of $(NHC)Rh(CO)_2Cl$ complexes confirming the *cis* geometry of all Rh(I) complexes (Scheme 1) and allowing the determination of TEP values (Table 1), which are in the same range (2052.6–2053.4 cm^{-1}) and similar to the TEP value of **IMe** (2053.0 cm^{-1}). These data show that the localization of the porphyrin has no or very weak inductive effect on the NHCs. Likewise, porphyrins exert similar inductive electronic effects, irrespective of the nature of the inner metal M^1 used in this study (M^1 = 2H, Ni or Zn). It is thus reasonable to consider that all NHCs presented here transfer similar amounts of electron density to Rh(I).

Steric pressures exerted by NHCs in the primary coordination sphere of Rh(I) were assessed by calculating their $\%V_{Bur}$ values and their steric maps to figure out ligands anisotropy. For this purpose, DFT calculations were first performed to optimize geometries of complexes **M^1-A-Rh(cod)Cl**, **M^1-B-Rh(cod)Cl** and **M^1-C-Rh(cod)Cl** (see ESI†). Then, $\%V_{bur}$ values (Table 1) and steric maps presenting the buried space around Rh(I) along the C_{NHC}–Rh(I) axes (Fig. 2 and ESI†) were calculated with Samb*V*ca 2.1.[12] NHCs **M^1-A** have $\%V_{bur}$ values in the range of 30.9–31.0% (Table 1, entries 2–4), but these values should be taken with caution since steric pressure is due to benzyl groups (yellow-orange area on the left side of **Ni-A** in Fig. 2). Indeed, only one conformation is used to calculate $\%V_{bur}$ values and steric maps, but benzylic sp^3 carbon atoms ensure enough flexibility to adapt the steric bulk and

Table 1 Electronic, steric and catalytic properties

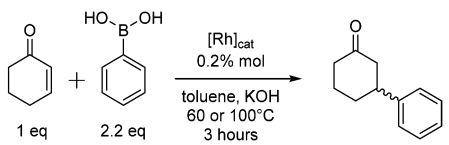

Entry	NHC ligand	TEP[a] (cm^{-1})	$\%V_{bur}$[b]	% conv.[c] (% yield) 60 °C	% conv.[c] (% yield) 100 °C
1	**IMe**	2053.0	26.0	41 (40)	63 (58)
2	**2H-A**	2052.6	31.0	38 (26)	55 (38)
3	**Zn-A**	2053.4	31.0	37 (27)	51 (45)
4	**Ni-A**	2053.4	30.9	38 (25)	56 (44)
5	**2H-B**	2053.0	26.9	30 (19)	45 (34)
6	**Zn-B**	2052.6	27.0	37 (33)	55 (51)
7	**Ni-B**	2053.4	26.8	33 (26)	52 (46)
8	**2H-C**	2053.4	32.4	14 (4)	46 (35)
9	**Zn-C**	2052.6	31.5	13 (7)	58 (52)
10	**Ni-C**	2053.0	32.0	12 (1)	91 (87)

[a] ν(CO) (cm^{-1}) measured in CH_2Cl_2 and TEP values calculated using the equation: TEP = 0.8001 × ν^{av}(CO) + 420 cm^{-1}, see ref. 10. [b] $\%V_{bur}$ values calculated with the Samb*V*ca 2.1 tool and the standard inputs given in Fig. 3. [c] Reaction conditions: 0.5 mmol of cyclohexen-2-one, 1.1 mmol of phenylboronic acid and 0.09 mmol of KOH in 2 mL of toluene with 0.2% mol catalyst loading, 60 or 100 °C, under argon. Conversions (% conv.) and yields (% yield) after 3 hours were determined by gas chromatography (GC) using anisole as internal standard and are the average values of three independent and reproducible experiments.

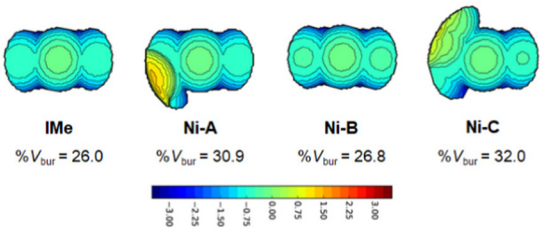

Fig. 2 Steric maps and %V_{bur} values of NHCs **IMe**, **Ni-A**, **Ni-B** and **Ni-C** calculated with SambVca 2.1 with the following standard inputs: bondi radii 1.17 Å, Rh–C_{NHC} 2.00 Å, r_{sphere} = 3.50 Å, mesh spacing 0.10 Å, H atoms excluded, see ref. 11.

conformations with %V_{bur} as low as ~26.5% are possible.[13] NHCs **M^1-B** possess %V_{bur} values in the range of 26.8–27.0% (Table 1, entries 5–7) and similar to the %V_{bur} value of NHC **IMe** (26.0%). Steric maps of NHCs **M^1-B** and **IMe** are similar because the steric pressure is due to the two *N*-methyl groups of the NHCs (see **Ni-B** and **IMe** in Fig. 2).

As expected, NHCs **M^1-C** with porphyrin wingtips are more bulky with %V_{bur} in the range of 31.5–32.4% (Table 1, entries 8–10). The broad greenish areas on the left side of their steric maps are due to the porphyrin cores (see **Ni-C** in Fig. 2). Thus, it is clear that porphyrins exert similar steric pressure in the primary coordination sphere of Rh(I), irrespective of the nature of the inner metal M^1 used in this study (M^1 = 2H, Ni or Zn). However, M^1 may impact the secondary coordination sphere of Rh(I) by modifying the shape of the porphyrin core.[14] To illustrate this point, DFT optimized structures of complexes **M^1-C-Rh(cod)Cl** are represented in Fig. 3. Porphyrins of complexes **2H-C-Rh(cod)Cl** and **Zn-C-Rh(cod)Cl** are rather flat (free base porphyrin is slightly saddle-shaped), while Ni(II) porphyrin in complex **Ni-C-Rh(cod)Cl** adopts a ruffled distortion in agreement with X-ray structures of similar NHCs reported by Ruppert, Weiss and coworkers.[15] It is also noticeable that the ruffled distortion of the porphyrin has two major consequences: the Ni(II) porphyrin wraps the Rh(I) complex along its C5–C15 axis and both metal ions get closer. Indeed, the Rh–Ni distance of ~5.08 Å in complex **Ni-C-Rh(cod)Cl** is slightly shorter than the Rh–Zn distance of ~5.25 Å in complex **Zn-C-Rh(cod)Cl** (Fig. 3).

Catalytic properties of (NHC)Rh(cod)Cl complexes were investigated in the conjugate addition of phenylboronic acid to cyclohexen-2-one.[16] Reactions were performed for 3 hours in toluene at 60 and 100 °C in the presence of KOH and catalyst loading of 0.2 mol% (Table 1), and were monitored by GC and UV-vis absorption spectroscopy (see ESI†). We observed that complexes **IMe-Rh(cod)Cl** (entry 1), **M^1-A-Rh(cod)Cl** (entries 2–4) and **M^1-*B*-Rh(cod)Cl** (entries 5–7) afforded rather similar reaction outcomes and time profiles (see ESI†), although slightly better conversion and yield were obtained with **IMe-Rh(cod)Cl**. Thus, porphyrins and their inner metal ions have no or very weak influence on the catalytic properties of the corresponding Rh(I) complexes. It can be explained by the fact that NHCs **IMe**, **M^1-A** and **M^1-B** possess similar electronic properties. Likewise, steric properties of NHCs **IMe** and **M^1-B** are also very similar. In the case of NHCs **M^1-A**, flexibility is ensured by benzylic sp^3 carbon atoms to adapt the steric bulk (*vide supra*) and porphyrins are too far from Rh(I) complexes to modulate the catalytic activity.

Interesting catalytic properties were observed for the three complexes **M^1-C-Rh(cod)Cl** (Table 1, entries 8–10). At 60 °C, they are significantly less active compared to the other catalysts (lower conversions and yields) and it may be attributed to the stronger steric pressure induced by the porphyrin wingtips. At 100 °C, catalytic activity of complexes **M^1-C-Rh(cod)Cl** depends on the nature of M^1 in the order 2H < Zn < Ni (see time profiles of the reactions in Fig. 4(a)). Complex **Ni-C-Rh(cod)Cl** is surprisingly more active with conversion and yield of 91% and 87%, respectively (Table 1, entry 10). This complex is approximately two times more active than complex **2H-C-Rh(cod)Cl**. Rate enhancement is only observed when the Ni(II) porphyrin is used as NHC wingtip. Indeed, there is no significant rate enhancement if the Ni(II) porphyrin and the NHC are not connected together (see reaction catalysed by **IMe-Rh(cod)Cl** + **NiP** *vs.* reaction catalysed by **IMe-Rh(cod)Cl** alone in the ESI†) or if they are connected but distant from each other.

Thermodynamic stability of complexes **2H-C-Rh(cod)Cl** and **Ni-C-Rh(cod)Cl** presenting the lowest and highest catalytic activities, respectively, was investigated. For this purpose, they were treated with KOH (100 eq.) in toluene at 100 °C and reaction mixtures were analyzed by $^{13}C\{^1H\}$ NMR spectroscopy (see ESI†). Complex **2H-C-Rh(cod)Cl** is stable and no significant change could be observed after 3 hours. Its lower catalytic

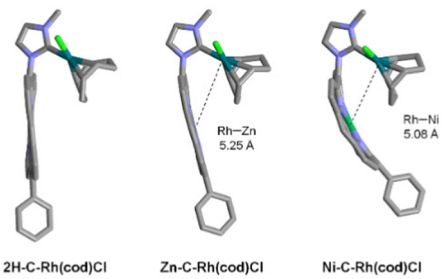

Fig. 3 DFT optimized structures of complexes **M^1-C-Rh(cod)Cl** with M^1 = 2H, Zn and Ni (*meso p*-tolyl groups and H omitted for clarity).

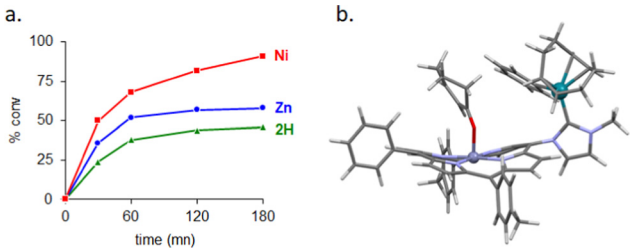

Fig. 4 (a) Time-dependant reaction profiles of the conjugate addition of phenylboronic acid to cyclohexen-2-one catalysed by **M^1-C-Rh(cod)Cl** (M^1 = Ni in red, Zn in blue and 2H in green) in toluene at 100 °C. (b) PM3-minimized molecular modelling of a plausible transition state of **Ni-C-Rh(cod)Cl** with phenyl and cyclohexen-2-one bonded to Rh(I) and Ni(II), respectively.

activity does not therefore seem to be due to its lower thermodynamic stability although its decomposition in the presence of the reaction substrates (phenylboronic acid and cyclohexen-2-one) cannot be totally excluded to explain the significant drop in catalytic activity after 1 hour. Complex **Ni-C-Rh(cod)Cl** is also stable for at least 30 minutes suggesting that its high initial catalytic activity is due to its kinetic activity. We also observed that complex **Ni-C-Rh(cod)Cl** slowly decomposed over time. Indeed, characteristic signals of carbene and cod ligands disappeared after 3 hours. This gradual decomposition may also explain the redshift of the Soret absorption band observed by UV-vis absorption spectroscopy after 1 hour reaction (see ESI†).

It is obvious that Ni(II) plays a significant role in the enhancement in the reaction rate, but this effect cannot be attributed to changes in inductive electronic effects or steric pressures exerted by NHCs, as previously shown. Although the exact mechanism of this cooperative effect between Rh(I) and Ni(II) remains unclear at this stage, we believe that the ruffled porphyrin core and the short Rh–Ni distance of $\sim$5 Å play significant roles in substrate-preorganization and reaction rate enhancement (Fig. 4(b)).[17] Extending the scope of the reaction to other substrates and detailed kinetic studies will further be needed to understand the exact role of Ni(II) in this reaction.

In summary, catalytic properties of molecular systems combining porphyrins and (NHC)Rh(cod)Cl complexes were investigated in the conjugate addition of phenylboronic acid to cyclohexen-2-one. Preliminary data show that catalytic activity of Rh(I) complexes is modulated by the metal in the porphyrin core when the macrocycle is used as NHC wingtip. In this case, we have shown that NHCs with free-base, Zn(II) and Ni(II) porphyrin wingtips transfer similar amount of electron density to Rh(I) and exert similar steric pressure in the primary coordination sphere of Rh(I). However, we found that Ni(II) in the porphyrin macrocycle dramatically increases the catalytic activity of the neighbouring Rh(I) complex. NHC-metal complexes with porphyrin wingtips are thus capable of cation-tunable reactivity and additional studies are underway to understand this phenomenon. Supramolecular catalysis and fine tuning of the catalytic activity of other NHC-metal complexes with porphyrins in close proximity are also actively explored in our group.[18,19]

We are grateful for the financial support of the French Agence Nationale de la Recherche (Grants ANR-19-CE07-0009 and ANR-19-CE07-0039), the University of Montpellier, the University of Rennes 1 and the Centre National de la Recherche Scientifique (CNRS). S. Scoditti is grateful for the financial support of Calabria Region (project POR Calabria-FSE/FESR 2014–2020).

Conflicts of interest

There are no conflicts to declare.

Notes and references

1 F. Glorius, N-Heterocyclic Carbenes in Catalysis – An Introduction, in, *N-Heterocyclic Carbenes in Transition Metal Catalysis. Topics in Organometallic Chemistry*, Springer, Berlin, Heidelberg, 2006, vol. 21; S. Díez-González, N. Marion and S. P. Nolan, *Chem. Rev.*, 2009, **109**, 3612–3676; P. de Frémont, N. Marion and S. P. Nolan, *Coord. Chem. Rev.*, 2009, **253**, 862–892; M. N. Hopkinson, C. Richter, M. Schedler and F. Glorius, *Nature*, 2014, **510**, 485–496; E. Peris, *Chem. Rev.*, 2018, **118**, 9988–10031.
2 D. G. Gusez, *Organometallics*, 2009, **28**, 6458–6461.
3 H. V. Huynh, *Chem. Rev.*, 2018, **118**, 9457–9492; S. Díez-González and S. P. Nolan, *Coord. Chem. Rev.*, 2007, **251**, 874–883; D. J. Nelson and S. P. Nolan, *Chem. Soc. Rev.*, 2013, **42**, 6723–6753; A. Gómez-Suárez, D. J. Nelson and S. P. Nolan, *Chem. Commun.*, 2017, **53**, 2650–2660.
4 J.-F. Longevial, C. Rose, L. Poyac, S. Clément and S. Richeter, *Eur. J. Inorg. Chem.*, 2021, 776–791.
5 J.-F. Lefebvre, M. Lo, J.-P. Gisselbrecht, O. Coulembier, S. Clément and S. Richeter, *Chem. – Eur. J.*, 2013, **19**, 15652–15660.
6 J.-F. Lefebvre, J.-F. Longevial, K. Molvinger, S. Clément and S. Richeter, *C. R. Chimie*, 2016, **19**, 94–102.
7 J. Trouve, P. Zardi, S. Al-Shehimy, T. Roisnel and R. Gramage-Doria, *Angew. Chem., Int. Ed.*, 2021, **60**, 18006–18013; P. Zardi, T. Roisnel and R. Gramage-Doria, *Chem. – Eur. J.*, 2019, **25**, 627–634.
8 J. S. Lindsey, I. C. Schreiman, H. C. Hsu, P. C. Kearney and A. M. Marguerettaz, *J. Org. Chem.*, 1987, **52**, 827–836.
9 J.-F. Lefebvre, D. Leclercq, J.-P. Gisselbrecht and S. Richeter, *Eur. J. Org. Chem.*, 2010, 1912–1920; C. H. Devillers, S. Hebié, D. Lucas, H. Cattey, S. Clément and S. Richeter, *J. Org. Chem.*, 2014, **79**, 6424–6434.
10 J.-F. Lefebvre, M. Lo, D. Leclercq and S. Richeter, *Chem. Commun.*, 2011, **47**, 2976–2978.
11 C. A. Tolman, *Chem. Rev.*, 1977, **77**, 313–348; A. R. Chianese, X. Li, M. C. Janzen, J. W. Faller and R. H. Crabtree, *Organometallics*, 2003, **22**, 1663–1667; T. Dröge and F. Glorius, *Angew. Chem., Int. Ed.*, 2010, **49**, 6940–6952; S. Wolf and H. Plenio, *J. Organomet. Chem.*, 2009, **694**, 1487–1492.
12 L. Falivene, Z. Cao, A. Petta, L. Serra, A. Poater, R. Oliva, V. Scarano and L. Cavallo, *Nat. Chem.*, 2019, **11**, 872–879.
13 $\%V_{bur}$ calculated with the X-ray crystal structure of a Rh(I) complex with 1-benzyl-3-methylimidazol-2-ylidene ligand in its coordination sphere, see the following reference: M. C. Cassani, M. A. Brucka, C. Femoni, M. Mancinelli, A. Mazzanti, R. Mazzoni and G. Solina, *New J. Chem.*, 2014, **38**, 1768–1779.
14 S. J. Kingsbury and M. O. Senge, *Coord. Chem. Rev.*, 2021, **431**, 213760.
15 J. Haumesser, J.-P. Gisselbrecht, J. Weiss and R. Ruppert, *Chem. Commun.*, 2012, **48**, 11653–11655; J. Haumesser, J.-P. Gisselbrecht, L. Karmazin-Brelot, C. Bailly, J. Weiss and R. Ruppert, *Organometallics*, 2014, **33**, 4923–4930.
16 B. J. Truscott, G. C. Fortman, A. M. Z. Slawin and S. P. Nolan, *Org. Biomol. Chem.*, 2011, **9**, 7038–7041; S. Ruiz-Botella and E. Peris, *ChemCatChem*, 2018, **10**, 1874–1881; I. Bratko, G. Guisado-Barrios, I. Favier, S. Mallet-Ladeira, E. Teuma, E. Peris and M. Gómez, *Eur. J. Org. Chem.*, 2014, 2160–2167; I. Peñafiel, I. M. Pastor, M. Yus, M. A. Esteruelas and M. Oliván, *Organometallics*, 2012, **31**, 6154–6161; C. Mejuto, G. Guisado-Barrios and E. Peris, *Organometallics*, 2014, **33**, 3205–3211; B. Ramasamy, A. P. Prakasham, M. K. Gangwar and P. Ghosh, *ChemistrySelect*, 2019, **4**, 8526–8533.
17 N. Abuhafez, A. Perennes and R. Gramage-Doria, *Synthesis*, 2022, A-I; M. Dommaschk, C. Schütt, S. Venkataramani, U. Jana, C. Näther, F. D. Sönnichsen and R. Herges, *Dalton Trans.*, 2014, **43**, 17395–17405; M. P. Byrn, C. J. Curtis, Y. Hsiou, S. I. Khan, P. A. Sawin, S. K. Tendick, A. Terzis and C. E. Strouse, *J. Am. Chem. Soc.*, 1993, **115**, 9480–9497.
18 L. Kovbasyuk and R. Krämer, *Chem. Rev.*, 2004, **104**, 3161–3187; C. G. Oliveri, P. A. Ulmann, M. J. Wiester and C. A. Mirkin, *Acc. Chem. Res.*, 2008, **41**, 1618–1629; M. J. Wiester, P. A. Ulmann and C. A. Mirkin, *Angew. Chem., Int. Ed.*, 2011, **50**, 114–137; M. Raynal, P. Ballester, A. Vidal-Ferran and P. W. N. M. van Leeuwen, *Chem. Soc. Rev.*, 2014, **43**, 1660–1733; M. Raynal, P. Ballester, A. Vidal-Ferran and P. W. N. M. van Leeuwen, *Chem. Soc. Rev.*, 2014, **43**, 1734–1787; V. Blanco, D. A. Leigh and V. Marcos, *Chem. Soc. Rev.*, 2015, **44**, 5341–5370; C. Yoo, H. M. Dodge and A. J. M. Miller, *Chem. Commun.*, 2019, **55**, 5047–5059; J. Trouve and R. Gramage-Doria, *Chem. Soc. Rev.*, 2021, **50**, 3565–3584.
19 Examples of porphyrin-based catalysts capable of inner metal-tunable reactivity: S. Yamaguchi, T. Katoh, H. Shinokubo and A. Osuka, *J. Am. Chem. Soc.*, 2007, **129**, 6392–6393; Y. Matano, K. Matsumoto, T. Shibano and H. Imahori, *J. Porphyrins Phthalocyanines*, 2011, **15**, 1172–1182; B. M. J. M. Suijkerbuijk, S. D. Herreras Martínez, G. van Koten and K. J. M. Klein Gebbink, *Organometallics*, 2008, **4**, 534–542.